Applied Nanoscience (2019) 9:945–956
https://doi.org/10.1007/s13204-018-0688-x

ORIGINAL ARTICLE

A new triple system DNA-Nanosilver-Berberine for cancer therapy

Anna Grebinyk[1,3] · Valeriy Yashchuk[2] · Nataliya Bashmakova[2] · Dmytro Gryn[2] · Tobias Hagemann[1] · Antonina Naumenko[2] · Nataliya Kutsevol[2] · Thomas Dandekar[3] · Marcus Frohme[1]

Received: 3 January 2018 / Accepted: 15 February 2018 / Published online: 3 March 2018

Abstract
The isoquinoline quaternary alkaloid Berberine possesses a variety of pharmacological properties that suggests its promising application for an anticancer delivery system design utilizing its ability to intercalate DNA. In the current work, we have investigated the effects of Berberine on the human T cell leukemia cell line in vitro. Fluorescent microscopy of leukemic cells revealed Berberine nuclear localization. The results showed that Berberine inhibited leukemic cell growth in a time- and dose-dependent manner, that was associated with reactive oxygen species production intensification and caspase 3/7 activity increase with followed apoptosis induction. Berberine was used as a toxic and phototoxic agent for triple system synthesis along with DNA as a carrier and nanosilver as a plasmonic accelerator of Berberine electronic transitions and high energy emission absorbent centers. The proposed method allows to obtain the complex of DNA with Berberine molecules and silver nanoparticles. The optical properties of free components as well as their various combinations, including the final triple system DNA-Nanosilver-Berberine, were investigated. Obtained results support the possibility to use the triple system DNA-Nanosilver-Berberine as an alternative therapeutic agent for cancer treatment.

Keywords Berberine · Apoptosis · Nanosilver · DNA delivery system

Introduction

The main steps of cancer chemotherapy include drug delivery to cancer cells, its intracellular accumulation and final implementation of drug toxicity against cancer cells due to the specific chemical reactions. The first generation of anticancer drugs for chemotherapy exploits the single toxic drug such as Doxorubicin (Tacar et al. 2013) and Cisplatin (Florea and Büsselberg 2011). The disadvantages of this approach include rather low selectivity and high general toxicity accompanied with the damage of blood vessels transporting drug. The next generation of anticancer drugs develops multicomponent systems combining drug with a special carrier, thus, achieving an enhanced selectivity, stability and circulation time. Due to the high biocompatibility and structural programmability, deoxyribonucleic acid (DNA) functions as an effective carrier for anticancer drugs, increasing its size as well as improving biodistribution and diminishing side effects (Jiang et al. 2012; Kang et al. 2015; Linko et al. 2015). Several strategies of using DNA as a carrier for common anticancer drug Doxorubicin in the form of polyplex (Kang et al. 2015), origami (Jiang et al. 2012), branched molecules in nanofilm (Cho et al. 2014) and nanogel linked by Cisplatin (Zhang and Tung 2017) were recently described. Doxorubicin was bound to the carrier via intercalation between DNA double helix base pairs. Such reversible and noncovalent binding of the toxic cargo and DNA carrier holds a big promise to exploit new alternative anticancer agents and to build DNA delivery nanosystem for application in cancer therapy.

Herbal secondary metabolites exhibit multiple biological and pharmacological properties, representing a natural library of bioactive compounds providing defense against herbivores, bacteria, fungi and viruses (Keasling 2008; Ortiz et al. 2014). Alkaloids, being one of the most versatile class of herbal secondary metabolites, include heterocyclic, nitrogen containing, low-molecular-weight molecules, frequently

✉ Anna Grebinyk
grebinyk.ann@gmail.com

[1] Technical University of Applied Sciences Wildau, Hochschulring 1, 15745 Wildau, Germany

[2] Taras Shevchenko National University of Kyiv, Volodymyrska 64, 01601 Kiev, Ukraine

[3] Biocenter, University of Würzburg, Am Hubland, 97074 Würzburg, Germany

with a high toxicity against other organisms (Keasling 2008; Xiao et al. 2012). The representatives of this class often exhibit pharmacological effects, leading to such tumor therapeutics as Vinblastine, Vincristine, Paclitaxel and Camptothecin (Mann 2002). The isoquinoline quaternary alkaloid Berberine ($C_{20}H_{19}NO_5$, 2,3-methylenedioxy-9,10-dimethoxyprotoberberine chloride, molecular weight of 353.36) promises applications as a low cost therapeutic due to the antiinflammatory, antimicrobial and antiviral activities (Ortiz et al. 2014; Cai et al. 2014). In recent years, Berberine has been reported to inhibit cell proliferation and to be toxic in vitro for many human cancer cell lines from different tumors such as FaDu (head and neck squamous cell carcinoma) (Seo et al. 2015), KB (oral cancer) (Kuo et al. 2005), PANC-1 and MIA-PaCa2 (pancreatic cancer) (Park et al. 2015), KM12C, KM12SM and KM12L4A (colon cancer) (Zhang et al. 2013), HL60 (leukemia) (Wu et al. 1999; Xiao et al. 2012), MCF-7 (breast cancer) (Patil et al. 2010), Ca Ski (cervical cancer) (Lin et al. 2007), PC-3 (prostate cancer) (Meeran et al. 2008) and WM793 (melanoma) (Serafim et al. 2008).

The potential intracellular targets of Berberine are DNA topoisomerase I, POT1 (Xiao et al. 2012), DNA Damage-Inducible Gene (Lin et al. 2007), Wnt (Albring et al. 2013, Zhang et al. 2013), p53 (Patil et al. 2010; Wang et al. 2014), NF-kB (Liu et al. 2010), cyclooxygenase-2 and Mcl-1 (Kuo et al. 2005), nucleophosmin/B23 (Wu et al. 1999), death-domain-associated protein (Zhang et al. 2010) as well as nucleic acids. Berberine has an ability to directly intercalate between DNA base pairs (Gumenyuk et al. 2012), leading to double-strand breaks (Wang et al. 2011, Li et al. 2013). Berberine was also shown to interact with human telomeric DNA quadruplex with a binding affinity of 10^6 M^{-1} (Arora et al. 2008) resulting in a significant stabilization through p–p interactions (Franceschin et al. 2006; Arora et al. 2008). Two Berberine molecules can herein be simultaneously stacked side-by-side onto the telomeric G-quadruplex (Bazzicalupi et al. 2013). The stabilization of intramolecular telomeric G-quadruplexes promotes selective downregulation of gene expression, DNA damage responses as well as telomerase inhibition (Neidle 2017). The resulting proliferation decrease suggests such a ligand-induced stabilization of the intramolecular telomeric G-quadruplexes as a new target for cancer therapy. Moreover, Berberine inhibits telomeric DNA binding with the POT1 protein (Xiao et al. 2012), an essential factor of the telomeres protection. Although, many results show that Berberine effectively binds DNA, suggesting its high nuclear affinity (Zhang et al. 2013), other data show Berberine mitochondrial localization (Pereira et al. 2007). Considerable attention focused on the mechanism of its anticancer cytotoxicity, showing mainly involvement of oxidative stress and mitochondrial dysfunction (Pereira et al. 2007; Meeran et al. 2008; Park et al. 2015), leading to apoptosis and cell cycle arrest (Kuo et al. 2005; Zhang et al. 2010; Patil et al. 2010; Cai et al. 2014).

In our study, we aimed to evaluate Berberine intracellular localization and its effects in human leukemic CCRF-CEM cells. For this purpose, we have estimated cell viability, reactive oxygen species (ROS) generation level and apoptosis induction in CCRF-CEM cells. We also proposed the system DNA-Nanosilver-Berberine that is the candidate to the novel generation of anticancer drugs due to the number of functional properties. DNA macromolecule plays the role of transporting carrier for Berberine molecules that can function as the main anticancer toxic agent. The system was designed considering the most recent study of Berberine photosensitizing activity (Andreazza et al. 2016). Surface plasmonic oscillation of fixed silver nanoparticles (AgNPs) (Basak et al. 2006; Muskens et al. 2007; Fang et al. 2008; Zhang et al. 2008; Yeshchenko et al. 2009; Ming et al. 2012) can be used to enhance electronic transitions of the Berberine molecules, intercalated in the DNA double helix. Besides this, the presence of silver nanoparticles in the proposed triple system gives the possibility to use it in the cancer radiotherapy as well (Hainfeld et al. 2004; Zheng et al. 2008). The complexation of silver nanoparticles with the DNA molecule is achieved via formation of silver nanoclusters along the DNA molecule (Kasyanenko et al. 2016). Therefore, the main purpose of silver nanoparticles here is to strength electronic transitions in Berberine molecules due to plasmonic resonance that gives the possibility to enhance its photosensitizing activity. The optical properties of system components alone as well as their various combinations, including the DNA-Nanosilver-Berberine system, were studied.

Methods

Chemicals

RPMI 1640 liquid medium, phosphate buffered saline (PBS), Fetal Bovine Serum (FBS), Penicillin/Streptomycin and L-gluthamine were obtained from Biochrom (Berlin, Germany). Berberine, Hoechst 33342 and 3-(4,5-dimethylthiazol-2-*yl*)-2,5-diphenyl tetrazolium bromide (MTT), silver nitrate ($AgNO_3$), sodium borohydride ($NaBH_4$) and DNA from chicken erythrocytes were obtained from Sigma Aldrich (St. Louis, MO, USA). Dimethylsulfoxide (DMSO) was purchased from Neolab (Heidelberg, Germany). Trypan blue was from Carl Roth GmbH + Co. KG (Karlsruhe, Germany).

Cell culture

The human T-cell leukemia cell line CCRF-CEM (ACC 240) was purchased from the Leibniz Institute DSMZ-German

Collection of Microorganisms and Cell Cultures. Cells were maintained in RPMI 1640 medium supplemented with 10% FBS, 1% Penicillin/Streptomycin and 2 mM L-gluthamine, using 25 cm^2 flasks at a 37 °C with 5% CO_2 in humidified incubator Binder (Tuttlingen, Germany). The number of viable cells was counted upon 0.1% trypan blue staining using Roche Cedex XS Analyzer (Basel, Switzerland).

Berberine accumulation in leukemic cells

CCRF-CEM cells were seeded at 2×10^5 cells/ml in 6-well plate Sarstedt (Nümbrecht, Germany) incubated for 24 h. Then cells were treated with 50 µM Berberine for 4 h, washed with PBS and stained with 10 µM Hoechst 33342 for 1 h. Live imaging of CCRF-CEM cells was performed with a Fluorescence Microscope Keyence BZ-9000 BIOREVO (Osaka, Japan) equipped with blue (λ excitation = 377 nm, λ emission = 447 nm) and green1 (λ excitation = 435 nm, λ emission > 515 nm) filters with the acquisition software Keyence BZ-II Viewer (Osaka, Japan). The merged images and single cell fluorescence intensity profiles were processed with the Keyence BZ-II Analyzer software (Osaka, Japan).

Cell viability

For cell viability assay, CCRF-CEM cells were cultured in 96-well cell culture plates Sarstedt (Nümbrecht, Germany) at 10^4i cells/well for 24 h. The cell culture medium was replaced by Berberine-contained medium. Cells were incubated in the presence of 0, 1, 3, 6, 12, 25, 50, 75, 100 and 150 µM Berberine for 24, 48 and 72 h. Cell viability was determined with a MTT reduction assay (Carmichael et al. 1987), during which 10 µL of MTT solution (5 µg/mL in PBS) was added to each well and incubated for 2 h at 37 °C degrees. The culture medium was replaced with 100 µL DMSO and after 15 min Diformazan formation was determined by measuring absorption at 570 nm with a microplate reader Tecan Infinite M200 Pro (Männedorf, Switzerland). Cell viability assay was accompanied with the phase contrast microscopy analysis of untreated and 25 µM Berberine treated CCRF-CEM cells with the Keyence BZ-9000 BIOREVO (Osaka, Japan). Curve fitting and calculation of the IC50 values were done using specialized software GraphPad Prism 7 (GraphPad Software Inc., USA). Briefly, individual concentration-effect curves were generated by fitting the logarithm of the tested compound concentration versus corresponding normalized percent of cell viability values using nonlinear regression.

Intracellular reactive oxygen species generation

Intracellular oxidative stress was quantified using fluorescent probe 2,7-dichlorofluorescin diacetate (DCFH-DA, Sigma-Aldrich Co., St-Louis, USA). CCRF-CEM cells were seeded into 96-well plates at 10^4 cells/well and incubated for 24 h. Cells were exposed to 0, 6, 12 and 25 µM Berberine-contained RPMI for 5 h, when 5 µM DCFH-DA was added and incubated for 40 min and fluorescence (λ excitation = 488 nm, λ emission = 520 nm) was detected with the microplate reader Tecan Infinite M200 Pro (Männedorf, Switzerland). At 50 min CCRF-CEM cells were observed using the Fluorescence Microscope Keyence BZ-9000 BIOREVO (Osaka, Japan) equipped with green2 filter (λ excitation = 472 nm, λ emission = 520 nm).

Caspase 3/7 activity

CCRF-CEM cells were seeded into 96-well plates at 10^4 cells/well and incubated for 24 h. The cell culture medium was replaced with fresh medium containing 25 µM Berberine. After 0–8 h the enzymatic activity of caspase 3/7 was determined of using the Promega Caspase-Glo® 3/7 Activity assay kit (Madison, USA) according to the manufacturer's instructions. Briefly, an equal volume of Caspase-Glo 3/7 reagent was added and gently mixed at 300 rpm for 1 min. The plate was then incubated at room temperature (RT) for 2 h. The luminescent signal, proportional to the amount of caspase activity present in the sample, was measured with the microplate reader Tecan Infinite M200 Pro (Männedorf, Switzerland). The caspase 3/7 activity of Berberine-treated cells was calculated as caspase activity relative to that in untreated cells.

Flow cytometry analysis

CCRF-CEM cells were seeded onto 6-well plates at a cell density of 2×10^5cells/well in 2 mL of culture medium and after 24 h were treated with 0, 6, 12 and 25 µM Berberine. Following a 24 h incubation period, the cells were analyzed with flow cytometry consequently to the double staining with an Annexin V-fluorescein isothiocyanate (FITC) and propidium iodide (PI) apoptosis detection kit (eBioscience™, San Diego, USA) according to the manufacturer's instructions. Briefly, cells were harvested, pelleted by centrifugation, washed in PBS and Binding buffer and resuspended in Binding buffer. FITC-conjugated Annexin V was added to the cells, incubated for 15 min at RT preventing light exposure. Cells were washed in Binding buffer and then propidium iodide was added to the cells. After 10 min cell suspension was analyzed with flow cytometry (BD FACSJazz™, Singapore). Viable cells were not stained (Annexin-FITC and PI negative), whereas dead cells exhibited Annexin-FITC negative and PI positive fluorescence. Annexin V-FITC positive, PI negative cells were considered in the early stage of apoptosis, both Annexin V- and PI-positive—in the late stage of apoptosis. A minimum

of 20,000 cells per sample were acquired and analyzed with the BD FACS™ software (Singapore).

Preparation of double DNA-Nanosilver and triple DNA-Nanosilver-Berberine preparation

AgNPs were synthesized in situ in aqueous solution DNA by reduction of precursor—silver nitrate ($AgNO_3$).

Double nanosystem synthesis

2 mL of a 0.1 M $AgNO_3$ aqueous solution was added to 5 mL of aqueous DNA solution ($C = 10^{-3}$ g/cm^3) and stirred for 20 min. Then, 2 mL of 0.1 M aqueous solution of reductant sodium borohydride ($NaBH_4$) was added. The final aqueous solution was stirred for 20 min. It turned reddish brown, thus, the formation of AgNPs was indicated.

Triple nanosystem synthesis

0.1 M $AgNO_3$ aqueous solution was added to 5 mL of aqueous DNA solution ($C = 10^{-3}$ g/cm^3) and stirred during 20 min. Then, 0.1 M aqueous solution of reductant $NaBH_4$ was added. The final aqueous solution was stirred for 20 min. Finally, the Berberine sulphate solution was injected to the prepared silver nanoparticle solution synthesized in DNA matrix and mixture was stirred additionally for 20 min. Added amount of 0.1 M $AgNO_3$ for triple nanosystem preparation was varied from 0.08 to 0.8 mL, amount of Berberine sulphate—from 0.5 to 1.5 mL.

Optical absorption spectra

For spectral measurements of free component as well as nanoparticle-containing systems a spectrofluorimeter Cary Eclipse (Varian, Austria) and Specord UV VIS (Jena, Germany) were used.

Statistical analysis

The data were represented as the mean ± standard deviation from a minimum of four independent experiments. The two-tailed Student's *t* test was used to analyze differences between controls and treated samples. Differences values $p < 0.05$ were considered to be significant. Data processing and plotting were performed using specialized application GraphPad Prism 7 (GraphPad Software Inc., USA).

Results and discussion

Biological activity of Berberine in vitro

Berberine accumulation in leukemic cells

To determine intracellular localization of Berberine is important to explain its anticancer activity since the location could give insights about drug's impact on cell metabolism. Berberine absorbs blue and emits green light, suggesting fluorescent microscopy. Exposure of CCRF-CEM cells to 50 μM Berberine for 4 h resulted in intracellular green fluorescence (Fig. 1a), suggesting its effective intracellular accumulation. Simultaneously cells were subjected to the live-staining with the blue-fluorescent DNA-binding dye Hoechst 33342. The single cell fluorescence intensity profiles were estimated for 150 pixels along yellow lines, pointed on the image "Merged" of CCRF-CEM, treated with 50 μM Berberine. The obtained fluorescence intensity profiles showed that the green fluorescence signal from Berberine entirely mimicked Hoechst 33342 blue signal distribution (Fig. 1b), demonstrating that Berberine was concentrated in the cell nucleus. Obtained data suggest that 50 μM Berberine binds DNA of CCRF-CEM upon in vitro conditions, what could be linked with its anticancer activity (Franceschin et al. 2006; Arora et al. 2008; Wang et al. 2011; Li et al. 2013; Ortiz et al. 2014). Previously, it was shown that Berberine is transferred into the nucleus via passive diffusion (Zhang et al. 2013), but in the concentrations less than 50 μM is selectively accumulated by mitochondria (Pereira et al. 2007; Serafim et al. 2008), pointing out on the multiphase model of Berberine accumulation.

Cell viability

A considerable attention has been paid to identify Berberine inhibiting potential on cancer cell viability (Kuo et al. 2005; Lin et al. 2007; Meeran et al. 2008; Patil et al. 2010; Zhang et al. 2010; Xiao et al. 2012; Zhang et al. 2013; Park et al. 2015; Seo et al. 2015). The viability of CCRF-CEM cells, exposed to Berberine at concentration ranging from 0 to 150 μM, was monitored within 72 h of incubation. Cell viability was estimated with MTT assay and expressed as % of untreated control cells (Fig. 2a). Berberine has shown a dose- and time-dependent toxicity against CCRF-CEM cells. Berberine concentration of 3, 6, 12, 25 and 50 μM induced cytotoxicity, directly proportional to the incubation time. CCRF-CEM cells under action of 25 μM Berberine showed the viability in 42, 19 and 11% of untreated control cells at 24, 48 and 72 h,

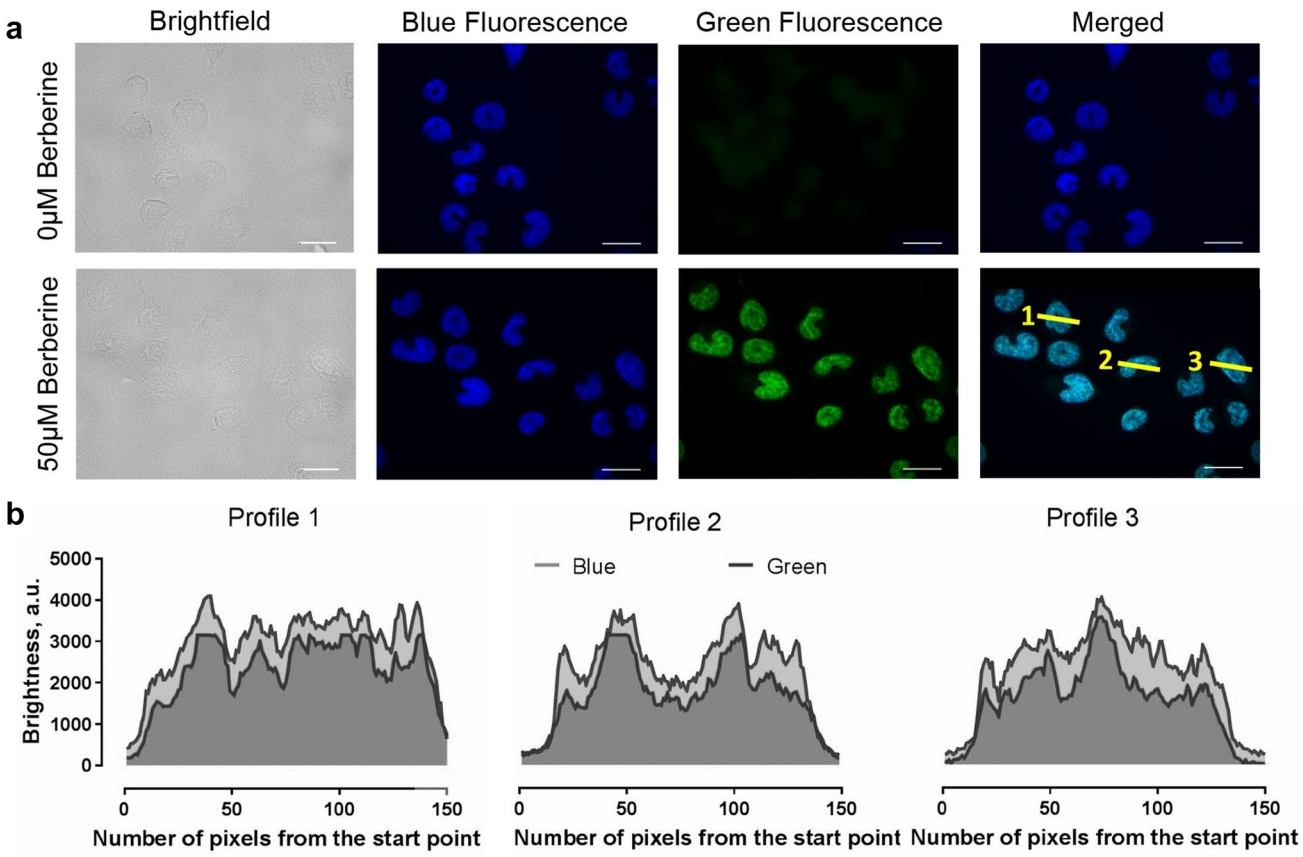

Fig. 1 Berberine intracellular localization: **a** – bright field and fluorescence (blue: λ excitation = 377 nm, λ emission = 447 nm, green1: λ excitation = 435 nm, λ emission > 515 nm) images of CCRF-CEM cells, incubated for 4 h with 50 μM Berberine, scale bar 20 μm, **b** – Single cell fluorescent profile along yellow lines 1, 2 and 3, pointed on the "Merged" fluorescence image

respectively. The highest tested Berberine concentrations (100 and 150 μM) had an acute cytotoxic effect at all time-points with no detectable cell viability. As shown on Fig. 2b, half-maximal inhibitory concentration (IC50) of Berberine was estimated to be 22 ± 5, 9 ± 1 and 5 ± 1 μM at 24, 48 and 72 h, respectively. Visual changes in cell quantity and morphology were also observed with the phase-contrast microscopy. As shown on Fig. 2c, 25 μM Berberine-treated cells demonstrated a decrease of viable cells along an incubation time from 0 to 72 h. Our results demonstrate that Berberine exhibits significant cytotoxic effects against human leukemic cells.

Intracellular reactive oxygen species generation

A high generation of reactive oxygen species promotes severe cellular damage causing cell death. Oxidative stress induction presents a promising anticancer strategy due to the high sensitivity of cancer cells to ROS level increase (Gorrini et al. 2013). The intracellular level of generated ROS in CCRF-CEM cells after 5 h exposure to 0–25 μM Berberine was estimated by an oxidative-sensitive fluorescence dye DCFH-DA (Myhre et al. 2003; Eruslanov and Kusmartsev 2010). DCFH-DA is able to penetrate into the cell, where it is deacyleted to the non-fluorescent form DCFH by intracellular esterases. Upon interaction of DCFH with intracellular ROS DCFH is oxidized to DCF, which is characterized by high green fluorescence. Consequently, the redox state of the sample can be monitored by detecting the fluorescence intensity (Eruslanov and Kusmartsev 2010). Increasing concentrations of Berberine administered to the cells provoked an increase in intracellular ROS generation—up to more than 100% (Fig. 3a2). In parallel an increase of the green fluorescence, proportionally to Berberine concentration, was observed with fluorescent microscopy (Fig. 3a1). Thus, we have shown that Berberine promotes oxidative stress in human leukemic cells by increasing intracellular ROS generation level, which is in accordance with previous findings (Pereira et al. 2007; Meeran et al. 2008; Park et al. 2015).

Apoptosis induction

Reactive oxygen species are increasingly recognized as important initiators and mediators of apoptosis suggesting

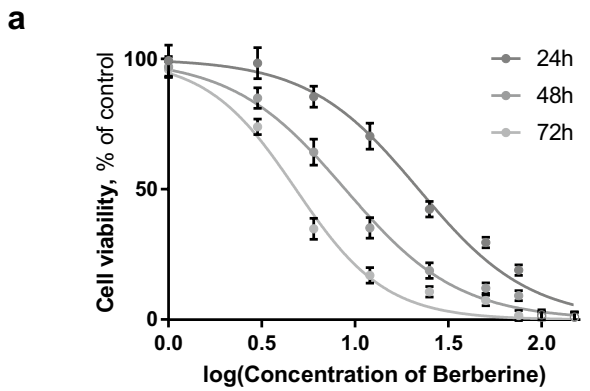

b

Time	IC50 (mean ± SD)
24h	22 ± 4 μM
48h	9 ± 1 μM
72h	5 ± 1 μM

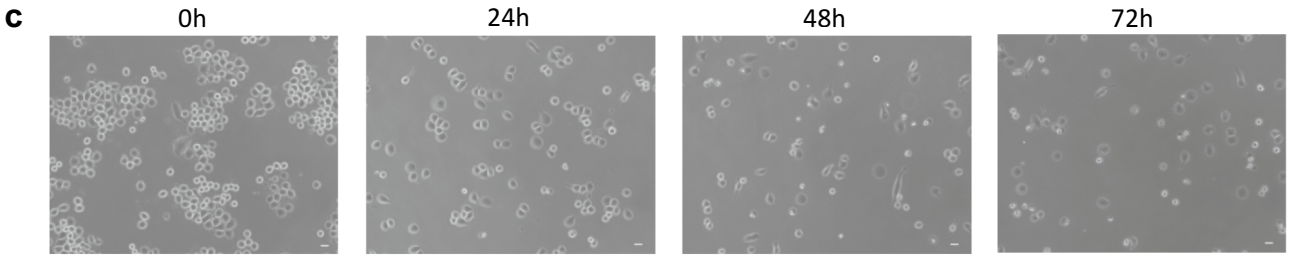

Fig. 2 Berberine action on cells: **a** – viability of CCRF-CEM cells, treated with 1-150 μM Berberine during 24-72 h, **b** – half maximal inhibitory concentration (IC50) of Berberine after 24 h, 48 h and 72 h exposure to CCRF-CEM cells, **C** – morphological characterization under phase contrast microscopy of CCRF-CEM cells, treated with 25 μM Berberine for 0-72 h, scale bar 20 μm

Fig. 3 Berberine proapoptotic effects: **a** – intracellular reactive oxygen species generation level of CCRF-CEM cells, exposured to 0, 6, 12 and 25 μM Berberine for 5 h: **1** – Fluorescence intensity of CCRF-CEM cells after 40 min incubation with DCFH-DA, **2** – Fluorescence microscopy of CCRF-CEM cells after 50 min incubation with DCFH-DA (green2: λ excitation = 472 nm, λ emission = 520 nm), scale bar 20 μm, **b** – Caspase 3/7 activity of CCRF-CEM cells, treated with 25 μM Berberine for 0-8 h

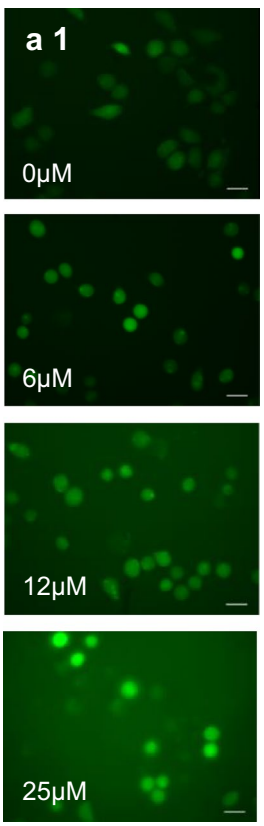

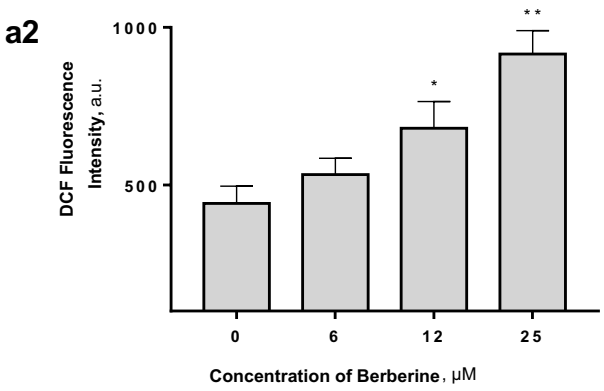

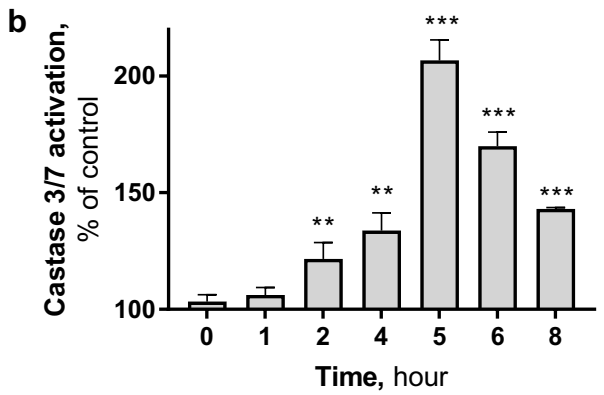

that Berberine could finally activate the caspase cascade. Therefore, we determined whether Berberine-induced cell-death is mediated through caspase-3/7. Treatment with 25 μM Berberine resulted in a time-dependent increase of the enzymes activity up to 210% (Fig. 3b), suggesting apoptotic death type mechanisms.

To investigate further the possible proapoptotic effect of Berberine, CCRF-CEM cells were subjected to double staining with Annexin V-FITC and propidium iodide. Protein Annexin V binds to phosphatidylserine which serves as an "eat me" signal on the cell-surface during apoptosis execution facilitating the phagocytic recognition and destruction of apoptotic cells (Suzuki et al. 2013). Flow cytometry analysis of double Annexin V-FITC/PI stained cells distinguish cells into four populations: viable (annexin V-FITC negative, PI negative), early apoptotic (annexin V-FITC positive, PI negative), late apoptotic (annexin V-FITC positive, PI positive) and dead (annexin V-FITC negative, PI positive) cells (Fig. 4a). A statistics summary report is illustrated in Fig. 4b. Untreated control cells showed high viability of 95%. 24 h incubation of CCRF-CEM cells with 6 μM Berberine resulted in apoptotic cell population growth up to 16% compared to 4% of control cells. Further Berberine concentration increase caused escalated appearance of both apoptotic and dead cells. The percentage of apoptotic cells treated with 12 and 25 μM Berberine were found to be 18 and 35%, and dead cells accounted 6 and 11% of the population, respectively. These finding support the suggested apoptotic cell death induction in leukemic cells under action of Berberine.

The system components spectral characterization

DNA

The optical properties of DNA are mainly determined by individual properties of π-electron systems of DNA bases that are dominant light absorbing centers in DNA molecule and practically are independent of each other. It is proven with similar absorption spectra of DNA and equimolar mixtures of low molecular model compounds—dAMP, dTMP, dCMP, dGMP (Yashchuk et al. 2007). Namely, these unique properties give the possibility to build the system of singlet and triplet electronic levels of DNA deliberately using the spectra of optical absorption, fluorescence and phosphorescence of the model compounds. It is appeared that the singlet levels of C acid and C base are the lowest ones among all. Therefore, due to energy

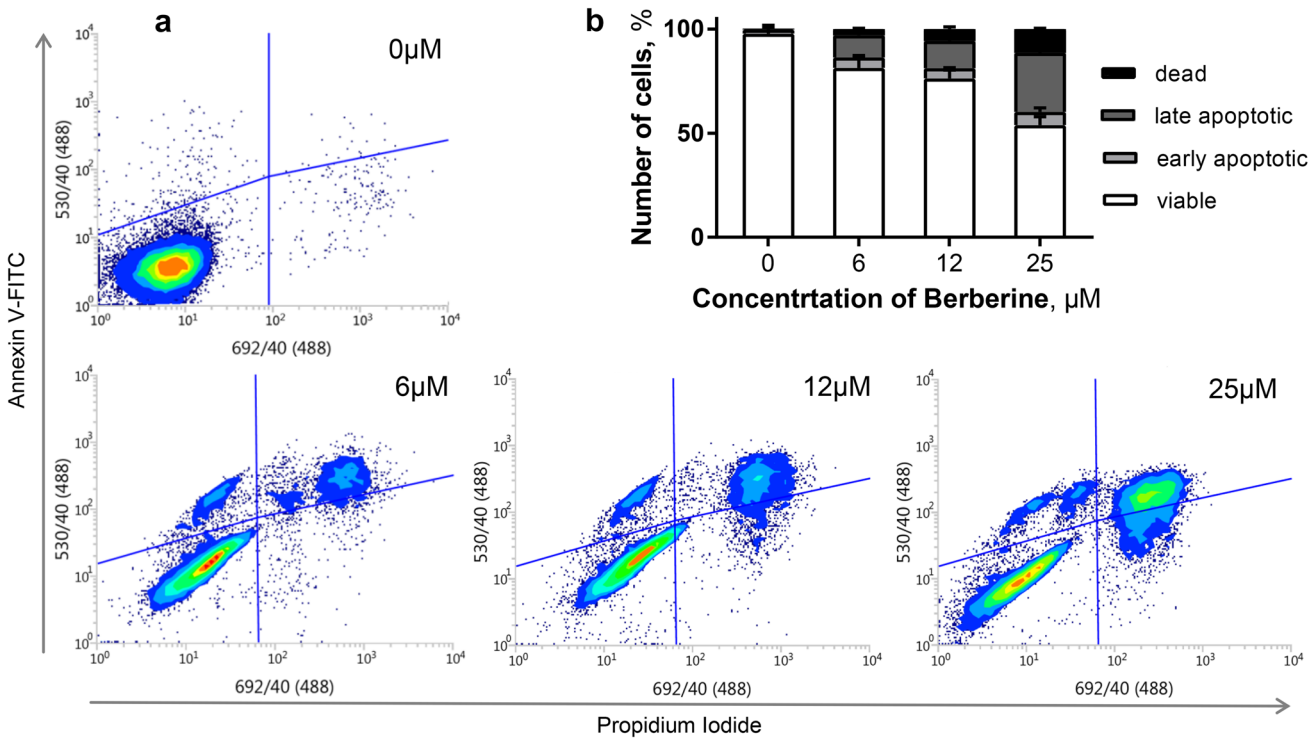

Fig. 4 Detection of apoptotic CCRF-CEM cells, treated with 0-25 μM Berberine, with Annexin V-FITC/PI double staining: **a** – in each panel the lower left quadrant shows negative cells for both PI and Annexin V-FITC— *viable*, upper left quadrant shows only Annexin V-FITC positive, PI negative cells— *early apoptotic*, and the upper right quadrant shows Annexin V-FITC and PI positive cells— *late apoptotic cells*, the lower right quadrant shows PI positive, Annexin V-FITC negative cells— *dead,* **b** – percentage of cell populations, differentiated with double Annexin-FITC/PI staining after treatment with Berberine

transfer between nucleic bases in the DNA macromolecule the fluorescence of DNA is determined by emission from C- and G- bases of DNA. As it was shown by Yashchuk et al. (2007), in fluorescent emission of DNA molecule the main contribution belongs to these species. Our measurements of DNA optical absorption spectra at RT, fluorescence and phosphorescence spectra at 77 K were found to be almost the same to obtained in other works (Yashchuk et al. 2007; Yashchuk and Kudrya 2017). The long-way band of DNA absorption located in the range 230-300 nm with the maximum 260 nm in wide temperature diapason including room temperature. At RT the DNA fluorescence intensity was weak with the quantum yield ~ 10^{-5}.

DNA-Berberine system

Optical absorption spectra The absorption spectrum of Berberine lies in the spectral range of $\lambda < 500$ nm, consisting four bands with the maxima at 420, 346, 263 and 227 nm. In the spectra of the mixture solutions of Berberine with DNA a substantial hypochromism up to 30% and the shift of maxima toward long waves were observed for 346 and 420 nm bands (Fig. 5a). The dipole moment of Berberine is oriented in the molecular plane (Danilov et al. 2006). If the dipole moments of molecules are oriented inparallel ("sandwich" structure), the spectra demonstrate hypochromism caused by the interaction between the π-systems of molecules that testifies to the intercalation or external stacking as probable binding mechanisms.

Fluorescence spectra The fluorescence spectrum of Berberine possesses one band with a maximum at about 550 nm. The fluorescence quantum yield of Berberine is very low (0.046) at room temperature (Maiti and Kumar 2007). The DNA addition to the Berberine solution increased its fluorescence intensity up to a factor of 200 (depending on the excitation λ, the concentration and the specimen type) and a maxima shift toward short waves in comparison with a free Berberine (Fig. 5b). The changes in the fluorescence spectra are caused by the fixation of Berberine molecules on the DNA matrix because of the probability of the radiationless excitation relaxation diminishes due to binding to DNA. Accordingly, the fluorescence quantum yield grows (Chalikian et al. 1994).

These spectral changes testified the binding of Berberine with DNA which is well consistent with the literature data (Maiti and Kumar 2007, Li et al. 2012). In our previous study, (Gumenyuk et al. 2012) we determined the binding parameters of Berberine to DNA: association constant $K = (5.2 \pm 0.2) \times 10^4$ M^{-1}, the number of binding sites occupied by one Berberine molecule $n = 1.85 \pm 0.1$, the parameter of cooperativity $\omega = 1.3 \pm 0.2$.

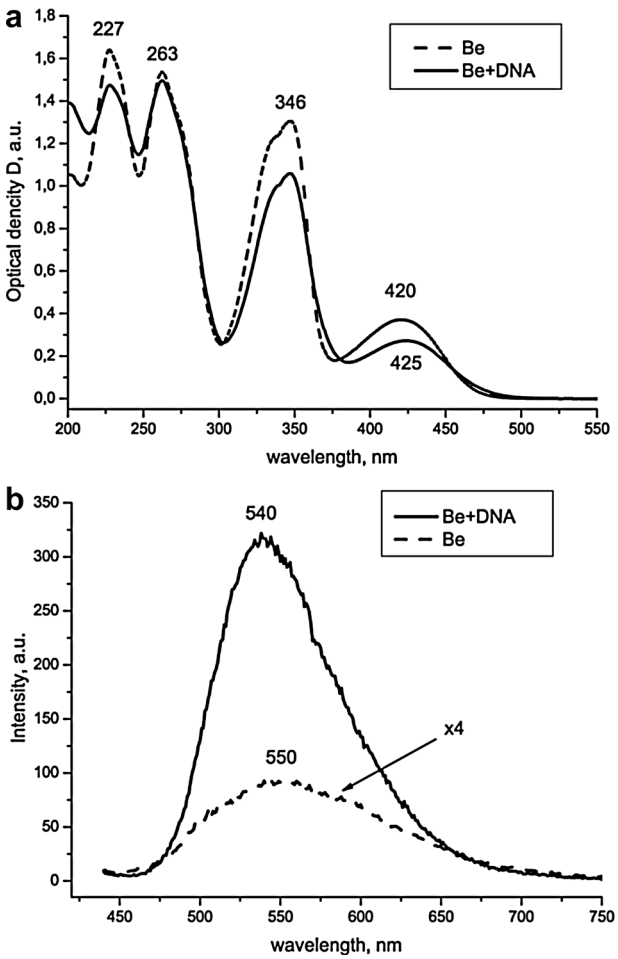

Fig. 5 DNA-Berberine system spectral characterization: **a** – absorption spectra of Berberine and Berberine + DNA aqueous solutions, Concentrations: C(DNA) = 22,28 × 10^{-3} mg/ml, C(Berberine) = 8,92 × 10^{-3} mg/ml, **b** – fluorescence spectra of Berberine and Berberine + DNA aqueous solutions. Concentrations: C(DNA) = 22,28 × 10^{-3} mg/ml, C(Berberine) = 8,92 × 10^{-3} mg/ml

DNA-Nanosilver system

Optical absorption spectra Absorption spectra of DNA-silver nanoparticle system in the spectral range of $\lambda < 700$ nm manifested itself by a broad band with maximum about 450 nm (Fig. 6a). According to Yeshchenko et al. (2009), this absorption is connected with surface plasmonic oscillation in silver nanoparticles. The shoulder at 260 nm in absorption spectra, to our opinion, belongs to DNA absorption contribution.

Fluorescence spectra Fluorescence spectra of aqueous solutions of DNA-AgNp systems possessed two spectral bands: long wave with maximum about 525 nm and short wave—with maximum about 350 nm (Fig. 6b). The centres responsible for emission band with maximum 525 nm could

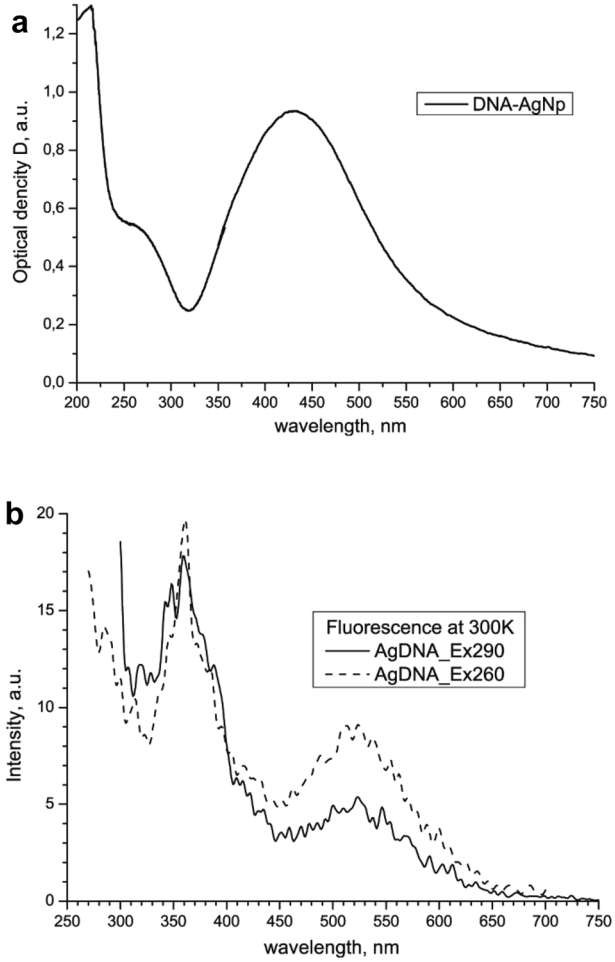

Fig. 6 DNA-Nanosilver system spectral characterization: **a** – absorption spectra of DNA-AgNp system in aqueous solutions at room temperature, C(DNA) = 0.011 × 10^{-3} M, **b** – DNA-Ag nanoparticle fluorescence spectra at T = 300 K in aqueous solutions, C(DNA) = 0.011 × 10^{-3} M

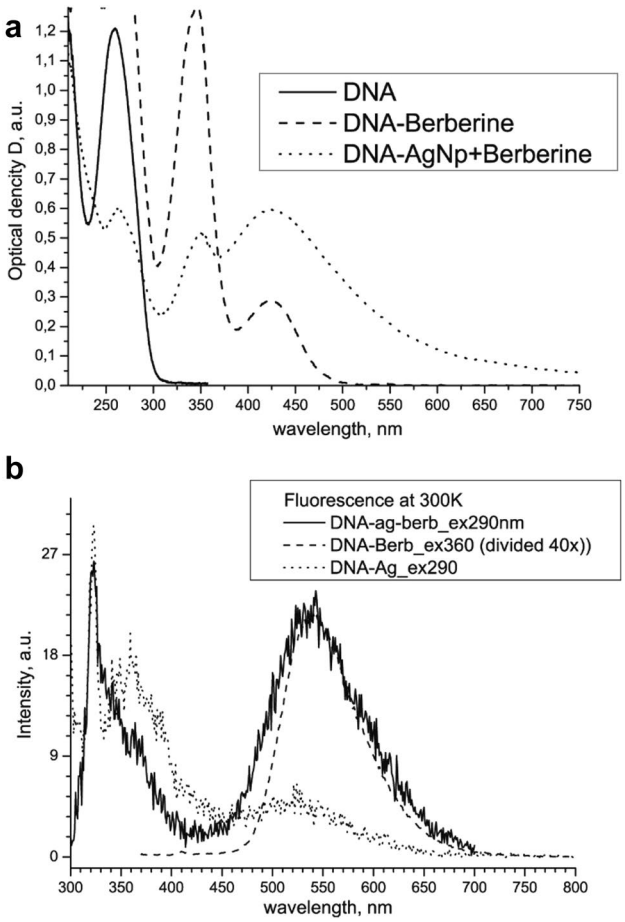

Fig. 7 DNA-Nanosilver-Berberine system spectral characterization: **a** – absorption spectra of DNA, DNA-Berberine and DNA-Nanosilver-Berberine system, Concentrations: C(DNA) = 0.067 mg/ml = 0.1 × 10^{-3}M, C(Berberine) = (0.0535 mg/ml = 1.6 × 10^{-4} M)/6 = 0.0089 mg/ml = 0.27 × 10^{-4} M, C(Berberine) = (0.0535 mg/ml = 1.6 × 10^{-4} M)/30 = 0.054 × 10^{-4} M, **b** – DNA-Nanosilver-Berberine, DNA-Berberine, and DNA-Nanosilver fluorescence spectra at T = 300 K

be connected with silver nanoclusters that were residues of Ag-nanoparticles synthesis (Xu and Suslick 2010; Dıez et al. 2012). Band with maximum 350 nm may be connected according to Yeshchenko et al. (2009) with radiative interband transitions strengthening by surface plasmonic oscillation. On the other hand, we do not exclude that this band belongs to DNA fluorescence, strengthening by silver nanoparticles. It is known that DNA practically exhibits no fluorescence at room temperature (Yashchuk and Kudrya 2017).

DNA-Nanosilver-Berberine system spectral characterization

Optical absorption spectra

As it shown in Fig. 7a, all three components of DNA-Ag nanoparticle-Berberine molecule system contributes in the total absorption spectrum. On the other hand, the dramatic changes in absorption of triple system comparing with the absorption of each component took place: we noticed the decreasing of DNA and Berberine long wave bands and domination of plasmonic band of Ag nanoparticles. This is the evidence of strong interaction between of components of the triple system.

Fluorescence spectra

In the spectral range more than 400 nm, the system DNA-Nanosilver-Berberine manifested one band with maximum 540 nm (Fig. 7b). The comparing of the fluorescence spectra of the triple nanosystem DNA-Ag nanoparticles-Berberine with fluorescence spectra of DNA-Berberine and DNA-Ag nanoparticles systems gives the possibility to conclude

that, namely, emission of Berberine molecules dominate in the total spectra. The short-wave fluorescent band with maximum 330-350 nm, to our opinion, belongs to radiative interband transitions in silver nanoparticles strengthening by surface plasmonic oscillation or DNA fluorescence accelerating by Ag nanoparticles.

Conclusion

Plants have versatile biological and medicinal properties, and are characterized by high safety, availability, accessibility and low cost, thus representing an invaluable source of chemicals with potential high therapeutic effects. Possessing a wide range of pharmacological actions, herbal alkaloid Berberine has driven a huge interest in cancer research.

In this context, the present study gives insights into the Berberine anticancer activity against human leukemic cells. Our findings indicate that Berberine accumulates in cell nucleus exhibiting high toxic effect against CCRF-CEM cell line. Under the treatment of CCRF-CEM cells with Berberine apoptotic death was induced by a mechanism, involving the reactive oxygen species production intensification and executive caspase 3/7 activation. Our findings highlight Berberine as an effective drug for leukemic cancer chemotherapy and as a promising candidate for the fast DNA-based delivery system synthesis via intercalation.

The spectral studies have shown that components of triple DNA-Nanosilver-Berberine system interact with each other and that these components are bound. The technology peculiarities of fabricated triple system strongly support this suggestion. DNA was proven to be a carrier for the delivery of Berberine molecules as a toxic and possibly phototoxic agent (Hirakawa and Hirano 2008; Hirakawa et al. 2012). Simultaneously, with silver nanoparticles, that have to play the role of accelerators of electronic transitions in the main active molecule of triple system—Berberine, as well as high energy emission absorbent centers in the case of its application in the combination with penetrative light radiation for deeper localized tumors (Hainfeld et al. 2004; Zheng et al. 2008). The fluorescence spectrum of triple system manifests the domination of Berberine molecules emission in the total spectra of fluorescence that gives the ground to conclude that the designed system holds a promise for its application in cancer therapy.

Acknowledgements Authors are grateful to the German Academic Exchange Service for the support (scholarship 57129429, Anna Grebinyk).

Author contributions The presented work was carried out in collaboration between all authors. YV, DT and FM coordinated the research work. GA estimated the leukemic cell viability, ROS production, Caspases 3/7 activity and Annexin staining, as well as performed the statistical analysis. HT performed fluorescent microscopy analysis. BN made spectral investigations of Berberine and Berberine-DNA system. GD performed spectral investigations of DNA-Nanosilver and DNA-Nanosilver-Berberine system. NA analyzed the spectral results. KN designed and synthesized the triple (DNA-Nanosilver-Berberine) system. GA and YV analyzed the data and wrote the manuscript. All authors discussed the results and commented on the manuscript.

Compliance with ethical standards

Conflict of interest The authors declare that they have no competing interests.

References

Albring KF, Weidemüller J, Mittag S, Weiske J, Friedrich K, Geroni MC, Lombardi P, Huber O (2013) Berberine acts as a natural inhibitor of Wnt/β-catenin signaling—identification of more active 13-arylalkyl derivatives. Biofact 39(6):652–662. https://doi.org/10.1002/biof.1133

Andreazza LN, Vevert-Bizet C, Bourg-Heckly G, Sureau F, Salvador JM, Bonneau S (2016) Berberine as a photosensitizing agent for antitumoral photodynamic therapy: insights into its association to low density lipoproteins. Int J Pharm 510(1):240–249. https://doi.org/10.1016/j.ijpharm.2016.06.009

Arora A, Balasubramanian C, Kumar N, Agrawal S, Ojha RP, Maiti S (2008) Binding of Berberine to human telomeric quadruplex—spectroscopic, calorimetric and molecular modeling studies. FEBS J 275:3971–3983. https://doi.org/10.1111/j.1742-4658.2008.06541.x

Basak D, Karan S, Mallik B (2006) Size selective photoluminescence in poly(methyl methacrylate) thin solid films with dispersed silver nanoparticles synthesized by a novel method. Chem Phys Lett 420:115–119. https://doi.org/10.1016/j.cplett.2005.12.062

Bazzicalupi C, Ferraroni M, Bilia AR, Scheggi F, Gratteri P (2013) The crystal structure of human telomeric DNA complexed with Berberine: an interesting case of stacked ligand to G-tetrad ratio higher than 1:1. Nucleic Acids Res 41:632–638. https://doi.org/10.1093/nar/gks1001

Cai Y, Xia Q, Luo R, Huang P, Sun Y, Shi Y, Jiang W (2014) Berberine inhibits the growth of human colorectal adenocarcinoma in vitro and in vivo. J Nat Med 68:53–62. https://doi.org/10.1007/s11418-013-0766-z

Carmichael J, Degraff WG, Gazdar AF, Minna JD, Mitchell JB (1987) Evaluation of a tetrazolium-based semiautomated colorimetric assay: assessment of chemosensitivity testing. Cancer Res 47:936–942. http://cancerres.aacrjournals.org/content/47/4/936.long

Chalikian TV, Plum GE, Sarvazyan AP, Breslauer KJ (1994) Influence of drug binding on DNA hydration: acoustic and densimetric characterizations of netropsin binding to the poly(dAdT).poly(dAdT) and poly(dA).poly(dT) duplexes and the poly(dT).poly(dA).poly(dT) triplex at 25 degrees C. Biochem 33:8629–8640. https://doi.org/10.1021/bi00195a003

Cho Y, Lee JB, Hong J (2014) Controlled release of an anti-cancer drug from DNA structured nano-films. Sci Rep 4:4078. https://doi.org/10.1038/srep04078

Danilov VI, Dailidonis VV, Hovorun DM, Kurita N, Murayama Y, Natsume T, Potopalsky AI, Zaika LA (2006) Berberine alkaloid: quantum chemical study of different forms by the DFT and MP2 methods. Chem Phys Lett 430(4–6):409–413. https://doi.org/10.1016/j.cplett.2006.09.026

Dıez I, Kanyuk MI, Demchenko AP, Walther A, Jiang H, Robin OI, Ras HA (2012) Blue, green and red emissive silver nanoclusters formed in organic solvents. Nanoscale 4:4434. https://doi.org/10.1039/C2NR30642E

Eruslanov E, Kusmartsev S (2010) Identification of ROS using oxidized DCFDA and flow-cytometry. Methods Mol Biol 594:57–72. https://doi.org/10.1007/978-1-60761-411-1_4

Fang Y, Seong NH, Dlott DD (2008) Measurement of the distribution of site enhancements in surface-enhanced Raman scattering. Science 321(5887):388–392. https://doi.org/10.1126/science.1159499

Florea AM, Büsselberg D (2011) Cisplatin as an anti-tumor drug: cellular mechanisms of activity, drug resistance and induced side effects. Cancers 3(1):1351–1371. https://doi.org/10.3390/cancers3011351

Franceschin M, Rossetti L, D'Ambrosio A, Schirripa S, Bianco A, Ortaggi G, Savino M, Schultes C, Neidle S (2006) Natural and synthetic G-quadruplex interactive Berberine derivatives. Bioorg Med Chem Lett 16(6):1707–1711. https://doi.org/10.1016/j.bmcl.2005.12.001

Gorrini Ch, Harris IS, Mak TW (2013) Modulation of oxidative stress as an anticancer strategy. Nat Rev Drug Discov 12:931–947. https://doi.org/10.1038/nrd4002

Gumenyuk VG, Bashmakova NV, Kutovyy SYu, Yashchuk VM, Zaika LA (2012) Binding parameters of alkaloids Berberine and sanguinarine with DNA. Ukr J Phys 56(62011):524–533. https://arxiv.org/abs/1201.2579

Hainfeld JF, Slatkin DN, Smilowitz HM (2004) The use of gold nanoparticles to enhance radiotherapy in mice. Phys Med Biol 49:309–315. https://doi.org/10.1088/0031-9155/49/18/N03

Hirakawa K, Hirano T (2008) The microenvironment of DNA switches the activity of singlet oxygen generation photosensitized by berberine and palmatine. Photochem Photobiol 84(1):202–208. https://doi.org/10.1111/j.1751-1097.2007.00220.x

Hirakawa K, Hirano T, Nishimura Y, Arai T, Nosaka Y (2012) Dynamics of singlet oxygen generation by DNA-binding photosensitizers. J Phys Chem B 116(9):3037–3044. https://doi.org/10.1021/jp300142e

Jiang Q, Song C, Nangreave J, Liu X, Lin L, Qiu D, Wang ZG, Zou G, Liang X, Yan H, Ding B (2012) DNA origami as a carrier for circumvention of drug resistance. J Am Chem Soc 134(32):13396–13403. https://doi.org/10.1021/ja304263n

Kang HC, Cho H, Bae YH (2015) DNA Polyplexes as combinatory drug carriers of doxorubicin and cisplatin: an in vitro study. Mol Pharm 12(8):2845–2857. https://doi.org/10.1021/mp500873k

Kasyanenko N, Varshavskii M, Ikonnikov E, Tolstyko E, Belykh R, Sokolov P, Bakulev V, Rolich V, Lopatko K (2016) DNA modified with metal nanoparticles: preparation and characterization of ordered metal-DNA nanostructures in a solution and on a substrate. J Nanomat. https://doi.org/10.1155/2016/3237250

Keasling J (2008) From yeast to alkaloids. Nat Chem Biol 4:524–525. https://doi.org/10.1038/nchembio0908-524

Li XL, Hu YJ, Wang H, Yu BQ, Yue HL (2012) Molecular spectroscopy evidence of Berberine binding to DNA: comparative binding and thermodynamic profile of intercalation. Biomacromol 13:873–880. https://doi.org/10.1021/bm2017959

Li J, Gu L, Zhang H, Liu T, Tian D, Zhou M, Zhou S (2013) Berberine represses DAXX gene transcription and induces cancer cell apoptosis. Lab Investig 93(3):354–364. https://doi.org/10.1038/labinvest.2012.172

Lin JP, Yang JS, Chang NW, Chiu TH, Su CC, Lu KW, Ho YT, Yeh CC, Mei-Dueyang, Lin HJ, Chung JG (2007) GADD153 mediates Berberine-induced apoptosis in human cervical cancer Ca Ski cells. Anticancer Res 27:3379–3386. https://ar.iiarjournals.org/content/27/5A/3379.long

Linko V, Ora A, Kostiainen MA (2015) DNA nanostructures as smart drug-delivery vehicles and molecular devices. Trends Biotechnol 33(10):586–594. https://doi.org/10.1016/j.tibtech.2015.08.001

Kuo CL, Chi CW, Liu, TY (2005) Modulation of apoptosis by Berberine through inhibition of cyclooxygenase-2 and Mcl-1 expression in oral cancer cells. In Vivo 19(1):247–252. http://iv.iiarjournals.org/content/19/1/247.long

Liu W, Zhang X, Liu P, Shen X, Lan T, Li W, Jiang Q, Xie X, Huang H (2010) Effects of Berberine on matrix accumulation and NF-kappa B signal pathway in alloxan-induced diabetic mice with renal injury. Eur J Pharmacol 638(1–3):150–155. https://doi.org/10.1016/j.ejphar.2010.04.033

Maiti M, Kumar GS (2007) Molecular aspects on the interaction of protoberberine, benzophenanthridine, and aristolochia group of alkaloids with nucleic acid structures and biological perspectives. Med Res Rev 27(5):649–695. https://doi.org/10.1002/med.20087

Mann J (2002) Natural products in cancer chemotherapy: past, present and future. Nat Rev Cancer 2:143–148. https://doi.org/10.1038/nrc723

Meeran SM, Katiyar S, Katiyar SK (2008) Berberine-induced apoptosis in human prostate cancer cells is initiated by reactive oxygen species generation. Toxicol Appl Pharmacol 229(1):33–43. https://doi.org/10.1016/j.taap.2007.12.027

Ming T, Chen H, Jiang R, Li Q, Wang J (2012) Plasmon-controlled fluorescence: beyond the intensity enhancement. J Phys Chem Lett 3(2):191–202. https://doi.org/10.1021/jz201392k

Muskens OL, Giannini V, Sánchez-Gil JA, Rivas JG (2007) Strong enhancement of the radiative decay rate of emitters by single plasmonic nanoantennas. Nano Lett 7(9):2871–2875. https://doi.org/10.1021/nl0715847

Myhre O, Andersen JM, Aarnes H, Fonnum F (2003) Evaluation of the probes 20,70-dichlorofluorescin diacetate, luminol, and lucigenin as indicators of reactive species formation. Biochem Pharmacol 65:1575–1582. https://doi.org/10.1016/S0006-2952(03)00083-2

Neidle S (2017) Quadruplex nucleic acids as targets for anticancer therapeutics. Nat Rev Chem 1:0041. https://doi.org/10.1038/s41570-017-0041

Ortiz LMG, Lombardi P, Tillhon M, Scovassi AI (2014) Berberine, an epiphany against cancer. Mol 9:12349–12367. https://doi.org/10.3390/molecules190812349

Park SH, Sung JH, Kim EJ, Chung N (2015) Berberine induces apoptosis via ROS generation in PANC-1 and MIA-PaCa2 pancreatic cell lines. Braz J Med Biol Res 48(2):111–119. https://doi.org/10.1590/1414-431X20144293

Patil JB, Kim J, Jayaprakasha GK (2010) Berberine induces apoptosis in breast cancer cells (MCF-7) through mitochondrial-dependent pathway. Eur J Pharmacol 645(1–3):70–78. https://doi.org/10.1016/j.ejphar.2010.07.037

Pereira GC, Branco AF, Matos JA, Pereira SL, Parke D, Perkins EL, Serafim TL, Sardão VA, Santos MS, Moreno AJ, Holy J, Oliveira PJ (2007) Mitochondrially Targeted Effects of Berberine (Natural Yellow 18, 5,6-dihydro-9,10-dimethoxybenzo(g)-1,3-benzodioxolo(5,6-a)quinolizinium) on K1735-M2 Mouse Melanoma Cells: comparison with Direct Effects on Isolated Mitochondrial Fractions. J Pharmacol Exper Ther 323(2):636–649. https://doi.org/10.1124/jpet.107.128017

Seo YS, Yim MJ, Kim BH, Kang KR, Lee SY, Oh JS, You JS, Kim SG, Yu SJ, Lee GJ, Kim DK, Kim CS, Kim JS, Kim JS (2015) Berberine-induced anticancer activities in FaDu head and neck

squamous cell carcinoma cells. Oncol Rep 34:3025–3034. https://doi.org/10.3892/or.2015.4312

Serafim TL, Oliveira PJ, Sardao VA, Perkins E, Parke D, Holy J (2008) Different concentrations of Berberine result in distinct cellular localization patterns and cell cycle effects in a melanoma cell line. Cancer Chemother Pharmacol 61:1007–1018. https://doi.org/10.1007/s00280-007-0558-9

Suzuki J, Denning DP, Imanishi EH, Horvitz R, Nagata Sh (2013) Xk-Related protein 8 and CED-8 promote phosphatidylserine exposure in apoptotic cells. Science 341(6144):403–406. https://doi.org/10.1126/science.1236758

Tacar O, Sriamornsak P, Dass CR (2013) Doxorubicin: an update on anticancer molecular action, toxicity and novel drug delivery systems. J Pharm Pharmacol 65(2):157–170. https://doi.org/10.1111/j.2042-7158.2012.01567.x

Wang Y, Kheir MM, Chai Y, Hu J, Xing D, Lei F, Du L (2011) Comprehensive study in the inhibitory effect of Berberine on gene transcription, including TATA box. PLoS One 6:e23495. https://doi.org/10.1371/journal.pone.0023495

Wang N, Zhu M, Wang X, Tan HY, Tsao SW, Feng Y (2014) Berberine-induced tumor suppressor p53 up-regulation gets involved in the regulatory network of MIR-23a in hepatocellular carcinoma. Biochimica Biophys Acta 9:849–857. https://doi.org/10.1016/j.bbagrm.2014.05.027

Wu HL, Hsu CY, Liu WH, Yung BY (1999) Berberine-induced apoptosis of human leukemia HL-60 cells is associated with down-regulation of nucleophosmin/B23 and telomerase activity. Int J Cancer. 81(6):923–929. https://doi.org/10.1002/(SICI)1097-0215(19990611)81:6<923::AID-IJC14>3.0.CO;2-D

Xiao N, Chen S, Ma Y, Qiu J, Tan JH, Ou TM, Gu LQ, Huang ZS, Li D (2012) Interaction of Berberine derivative with protein POT1 affect telomere function in cancer cells. Biochem Biophys Res Commun 419:567–572. https://doi.org/10.1016/j.bbrc.2012.02.063

Xu H, Suslick KS (2010) Water-soluble fluorescent silver nanoclusters. Adv Mater 22:1078–1082. https://doi.org/10.1002/adma.200904199

Yashchuk VM, Kudrya VYu (2017) The spectral properties of DNA and RNA macromolecules at low temperatures: fundamental and applied aspects. Method Appl Fluoresc 5:014001. https://doi.org/10.1088/2050-6120/aa50c9

Yashchuk VM, Kudrya VYu, Losytskyy MYu, Dubey IYA, Suga H (2007) Electronic excitation energy transfer in DNA. Nature of triplet excitations capturing centers. Mol Cryst Liq Cryst 467:311–323. https://doi.org/10.1080/15421400701224751

Yeshchenko OA, Dmitruk IM, Alexeenko AA, Losytskyy MY, Kotko AV, Pinchuk AO (2009) Size-dependent surface-plasmon-enhanced photoluminescence from silver nanoparticles embedded in silica. Phys Rev B 79:235438. https://doi.org/10.1103/PhysRevB.79.235438

Zhang W, Tung CH (2017) Sequence-independent DNA nanogel as a potential drug carrier. Macromol Rapid Commun 8(20):1700366. https://doi.org/10.1002/marc.201700366

Zhang A, Zhanga J, Fang Y (2008) Photoluminescence from colloidal silver nanoparticles. J Lumin 128(10):1635–1640. https://doi.org/10.1016/j.jlumin.2008.03.014

Zhang X, Gu L, Li J, Shah N, He J, Yang L, Hu Q, Zhou M (2010) Degradation of MDM2 by the interaction between Berberine and DAXX leads to potent apoptosis in MDM2-overexpressing cancer cells. Cancer Res 70(23):9895–9904. https://doi.org/10.1158/0008-5472.CAN-10-1546

Zhang J, Cao H, Zhang B, Cao H, XuX Ruan H, Yi T, Tan L, Qu R, Song G, Wang B, Hu T (2013) Berberine potently attenuates intestinal polyps growth in ApcMin mice and familial adenomatous polyposis patients through inhibition of Wnt signalling. J Cell Mol Med 17(11):484–1493. https://doi.org/10.1111/jcmm.12119

Zheng Y, Hunting DJ, Ayotte P, Sanche L (2008) Radiosensitization of DNA by gold nanoparticles irradiated with high-energy electrons. Radiat Res 169:19–27. https://doi.org/10.1667/RR1080.1